ELSEVIER

Thermochimica Acta 395 (2003) 3–19

thermochimica acta

www.elsevier.com/locate/tca

Determination of structural, thermodynamic and phase properties in the Na_2S–H_2O system for application in a chemical heat pump

R. de Boer, W.G. Haije*, J.B.J. Veldhuis

Energy Research Centre of the Netherlands, P.O. Box 1, 1755 ZG Petten, The Netherlands

Received 1 March 2002; accepted 6 March 2002

Abstract

Structural, thermodynamic and phase properties in the Na_2S–H_2O system for application in a chemical heat pump have been investigated using XRD, TG/DTA and melting point and vapour pressure determinations. Apart from the known crystalline phases $Na_2S{\cdot}9H_2O$, $Na_2S{\cdot}5H_2O$ and Na_2S a new phase $Na_2S{\cdot}2H_2O$ has been proven to exist. $Na_2S{\cdot}\frac{1}{2}H_2O$ is not a phase but a 3:1 mixture of Na_2S and $Na_2S{\cdot}2H_2O$, presumably stabilised by very slow dehydration kinetics. The vapour pressure–temperature equilibria of the sodium sulphide hydrates have been determined and a consistent set of thermodynamic functions for these compounds has been derived. XRD measurements indicate the topotactic character of the transitions between the hydration states.

Keywords: Sodium sulphide hydrate; Vapour pressure; Phase diagram; Thermodynamic properties; Heat pump

1. Introduction

The present concern about themes like greenhouse effect, pollution, renewable energy and durable society has incited researchers to find better ways of using the limited energy resources at our disposal. This resulted in the development of fuel cells, solar cells and heat pumps, to mention only a few. At the same time energy efficiency has a huge potential for reduction of energy consumption and CO_2 reduction. In the Netherlands alone about 100 PJ yr^{-1} (1 PJ (petajoule) = 10^{15} J) worth of industrial waste heat in the temperature range of 50–150 °C is actively cooled and dissipated into the environment. On an European scale this amounts to approximately 10 times this number [1]. In recent years much effort has been put into the development of heat driven solid-sorption chemical heat pumps and heat transformers [2] for heating as well as cooling purposes. The working principle of this apparatus is based on the exothermic absorption and endothermic desorption of vapour in solids, e.g. water in silica or zeolites [3], ammonia in metal salts [4] or in carbon [5]. The thermal effects and thus the attainable energy densities are much larger, about one order of magnitude, in the case of chemisorption, e.g. hydration of metal salts, than in the case of physisorption, e.g. water in silica. The present paper concerns the structural, thermodynamic and phase properties of the Na_2S–H_2O system that is to be used in a waste heat driven solid–vapour

* Corresponding author. Tel.: +31-224-564-790; fax: +31-224-5682-2615.
E-mail address: haije@ecn.nl (W.G. Haije).

0040-6031/02/$ – see front matter
PII: S0040-6031(02)00158-2

absorption heat pump for cooling purposes in buildings and industrial processes. The heat pump operation is based on the following equilibrium reaction:

$$Na_2S \cdot 5H_2O\,(s) \leftrightarrow Na_2S \cdot \tfrac{1}{2}H_2O\,(s) + 4\tfrac{1}{2}H_2O\,(g),$$
$$\Delta_r H \approx 300\,\mathrm{kJ\,mol^{-1}} \quad (1)$$

Preliminary tests with lab and bench scale heat pump units based on this solid–vapour pair yielded results that could not entirely be understood on the basis of the known literature on this system [6–9]. The most important feature being the fact that the amount of water after charging with a temperature difference between condenser and accumulator of about 60 °C was only about 66% of the expected value. When this temperature difference was raised to about 70 °C the rest of the water condensed. This suggested there should be another phase with a composition close to $Na_2S{\cdot}2H_2O$ present in the phase diagram, which had already been proposed by Andersson et al. [8,9] but was never proven as a fact. Therefore, experiments were performed to prove the existence of this new phase, to determine its p–T equilibrium line and to re-establish data already published in older literature [6–9] on the phase diagram and solid–vapour equilibria. Temperature dependent XRD was used to establish the number of crystallographic phases present in the system. DTA/TG was used to determine the amount of water released at each dehydration step and vapour pressure measurements were performed in order to establish the operational window for the heat pump and to derive the reaction enthalpy and entropy for the $Na_2S{\cdot}2H_2O \leftrightarrow Na_2S{\cdot}\frac{1}{2}H_2O$ transition.

It should be borne in mind, as will become clear in the following, that the hydration numbers 2 and $\frac{1}{2}$ should be interpreted as *'approximately* 2*'* and *'approximately* $\frac{1}{2}$*'*.

2. Materials and methods

2.1. Sample preparation

$Na_2S{\cdot}xH_2O$ (Merck, extra pure, about 35% Na_2S) was used as starting material for all of the experiments. The water content corresponds to approximately sodium sulphide nanohydrate, $Na_2S{\cdot}9H_2O$. For the preparation of the samples that were used in the experiments the starting material was dehydrated until the desired water content was reached. For dehydration a weighed amount of the starting material was placed in a glass container connected to a cold trap in liquid nitrogen and a vacuum pump. After evacuation of the system, water vapour from the starting material started to condense in the cold trap. The glass container with the starting material is heated to approximately 50 °C to accelerate the dehydration process. The colour of the sample changed during the dehydration from white/colourless to yellow when the amount of $Na_2S{\cdot}5H_2O$ in the sample increased. The resulting water content of the samples was calculated from the weight loss of the starting material. All handling of sodium sulphide was conducted as much as possible under protective nitrogen atmosphere, to prevent any reaction with oxygen and carbon dioxide in the air.

The composition of the samples used for the experiments was determined by weighing the remaining sodium sulphide hydrate after partial dehydration and then calculating the water content, assuming $Na_2S{\cdot}9H_2O$ to be the starting compound. Most samples were checked by X-ray powder diffraction for their composition. The measured diffraction patterns were critically compared to the known diffraction patterns of $Na_2S{\cdot}xH_2O$, where $x = 0$, 2, 5 and 9 [9–13]. In addition the diffraction patterns of Na_2SO_3 and Na_2S_2 were sometimes present at very low intensity ($I/I_{100} < 0.05$).

The samples used in the determination of the vapour pressure of sodium sulphide hydrate were also chemically analysed by titration for the presence of sulphide, sulphite and sulphate. All samples contained sulphide as the main component, a very small amount of sulphite and even less sulphate. The presence of these substances is considered not to influence the vapour pressure measurements, because mixing of the sulphide and the sulphite or sulphate does not occur [14].

2.2. Thermal analysis

Thermal analyses on samples of sodium sulphide hydrate were done to obtain information on the dehydration behaviour of $Na_2S{\cdot}xH_2O$. The goal was to determine temperatures at which dehydration reactions occur and to determine the heat of the reactions.

Table 1
Thermal properties of the standard materials used for calibration

Standard material	Mole weight (g mol^{-1})	$T_{transition}$ (°C)	$\Delta H_{transition}$ (J mol^{-1})	References
KNO_3	101.11	128	−5106	[15,16]
Sn	118.96	230	−7062	[15,16]
$KClO_4$	299.5	299	−13772	[15,16]
$RbNO_3$ (Alfa, puratronic)	147.47	166	−3923	[16]

The measurements were done using a Netzsch STA 409 TG/DTA apparatus. The system was calibrated prior to the measurement, using KNO_3, $RbNO_3$, $KClO_4$ and Sn, in order to determine the calorimetric sensitivity. A temperature calibration is part of the standard measurement procedure and was checked before the measurements using the same materials as for the calorimetric calibration (Table 1).

The standard measurement conditions were as given in Table 2. Sample pans were used either with or without a lid depending on the required mass transport of the water vapour out of the sample. The calorimetric sensitivity was determined at 0.31 ± 0.02 ($\pm 6\%$) $\mu V\,s\,mJ^{-1}$. The influence of changes in heating rate, sample weight, and helium flow rate on the calorimetric sensitivity were negligible.

For conducting controlled dehydration and rehydration reactions of sodium sulphide, the helium flow to the TG/DTA system was saturated with water vapour at 15 °C, resulting in a water vapour pressure of 17 mbar in helium. For these measurements the sample mass used was about 10 mg and apart from using 1.6 K min^{-1} the heating rate was also lowered to 0.4 K min^{-1}. In this way the measurements are performed under thermal equilibrium as much as possible and the influence of slow mass transfer processes on the measurements is minimised. Lower heating rates resulted in poor determination of the accompanying heat effects. These measurements were performed in pans without a lid.

Table 2
Standard measurement conditions for the analysis of the thermal dehydration of Na_2S–H_2O samples

Crucible material	Al_2O_3
Reference material	Al_2O_3
Average sample weight	5 mg
Heating rate (high)	1.6 K min^{-1}
Heating rate (low)	0.4 K min^{-1}
Atmosphere	Helium, 99.999% at a flow rate of 200 ml min^{-1}

2.3. X-ray powder diffraction

For the identification of the hydrates of sodium sulphide X-ray powder diffraction was applied, using a Guinier type camera. The samples were put in small polyethylene bags to prevent reactions with air or (de)hydration reactions during the measurement. The measured X-ray diffraction patterns were compared to the known patterns [10][1], [11–13] of the sodium sulphide–water system.

For a crystallographic study of the dehydration reaction of sodium sulphide hydrate a Guinier–Lenné type camera was used with Cu $K\alpha_{1,2}$ radiation, $\lambda = 1.5418$ Å. The sodium sulphide sample of about 50 mg was placed in the camera on a platinum grid in an atmosphere of helium and water vapour. The temperature of the sample or the water vapour pressure was varied, by changing the temperature of the saturator, in order to induce the desired dehydration or rehydration reactions. The diffraction pattern was recorded continuously while either changing the water vapour pressure in the camera or the sample temperature, thus inducing phase changes in the sample.

2.4. Phase diagram determination

DTA measurements were done for the determination of the melting temperatures in the part of the Na_2S–H_2O phase diagram relevant for practical heat pump operation. Samples of about 100 mg of

[1] [10] Tel.:+610-325-9814; fax: +610-325-9823, info@icdd.com

$Na_2S{\cdot}xH_2O$ $(0 < x < 5)$ were placed in small evacuated and sealed glass capsules (height 10 mm, diameter 8 mm) with a very thin polished bottom surface. The samples were heated three times at 1 °C min^{-1} to 130 °C and cooled with 1 °C min^{-1} to 20 °C and kept constant at that temperature for 2 h. An empty glass capsule was used as reference.

In addition visual melting point determinations were done in a temperature controlled water bath. Crystalline sodium sulphide hydrate was put in a tubular glass capsule (height 70 mm, diameter 4 mm) that was evacuated and sealed. The glass capsule was connected to a calibrated Pt100 temperature sensor and placed in the water bath that was heated at a rate of 3 °C h^{-1}. The melting temperature was determined visually at the point where crystallites started to soften and melt.

2.5. Vapour pressure measurements

The water vapour pressure of sodium sulphide hydrate as a function of its temperature was determined using a calibrated MKS Baratron 690A diaphragm type pressure sensor connected to a glass container (diameter 24 mm, height 50 mm) filled with the salt hydrate. The container with the salt was placed in a temperature controlled bath (Julabo, type HP 25, Germany), and its temperature was determined using a calibrated Pt100 temperature sensor connected to a Keithley multimeter. Calibration of the temperature sensor was performed using the same sample holder filled with Al_2O_3 powder in order to simulate the measurement conditions: estimated accuracy ±0.2 °C. The temperature sensor was positioned in an insert in the centre of the sample container. The pressure sensor was maintained at constant temperature of 45 °C to avoid temperature drift of the sensor during measurement and to avoid condensation of the water vapour in the sensor. The tubing of the measurement set-up was heated to 60 °C to prevent condensation of the water vapour. A high vacuum pump was connected to the system in order to evacuate the system prior to the measurement.

The temperature of the sample was changed stepwise approximately 10 °C after each measurement. When the temperature of the bath reached it pre-set temperature, it took approximately 15 min for the sample temperature to stabilise at this temperature. Only after stabilisation of the temperature of the sample a pressure reading was taken. Data were acquired both on stepwise heating and on cooling.

3. Results and discussion

3.1. Thermal analysis: measurements in a dry helium atmosphere

On heating a sample of $Na_2S{\cdot}9H_2O$ in a flow of helium the first dehydration step to $Na_2S{\cdot}5H_2O$ occurs readily in all samples, provided the heating rate is low, and there is no lid on the sample pan, so the mass transfer of water vapour is not limited. Already at room temperature dehydration to $Na_2S{\cdot}5H_2O$ occurs just by passing a dry helium flow over the sample. At high heating rates, or with a lid on the sample pan the melting temperature of $Na_2S{\cdot}9H_2O$ (49 °C) is reached before the first dehydration reaction has finished and a melting peak of the remaining $Na_2S{\cdot}9H_2O$ was seen in the DTA signal. In that case limited mass transfer of water vapour prevented the dehydration reaction to proceed fast enough. On further heating of the samples again a distinction could be made between measurements with water vapour transport limitation and without this limitation. When water vapour transport is limited the dehydration reaction of $Na_2S{\cdot}5H_2O$ to lower water content starts at 60 °C and stops between 90 and 100 °C, when (partial) melting of the sample occurs. The residual water content is then evaporated at approximately 180 °C. In the case water vapour transport is not limited the dehydration occurs under almost equilibrium conditions, $Na_2S{\cdot}5H_2O$ then first loses its water to $Na_2S{\cdot}2H_2O$ and then to Na_2S. Further heating to 300 °C does not give any further weight loss, indicating that the final composition is completely dehydrated solid Na_2S. The average enthalpy of the complete dehydration of $Na_2S{\cdot}5H_2O$ to Na_2S is $(3.1 \pm 0.2) \times 10^2$ kJ mol^{-1} of Na_2S.

3.2. Thermal analysis: measurements in a helium/water vapour atmosphere

The results of the TG/DTA experiments carried out in a flow of helium with 17 mbar water vapour pressure are shown in Fig. 1, where the DTA curve and the weight loss curve as a function of temperature for

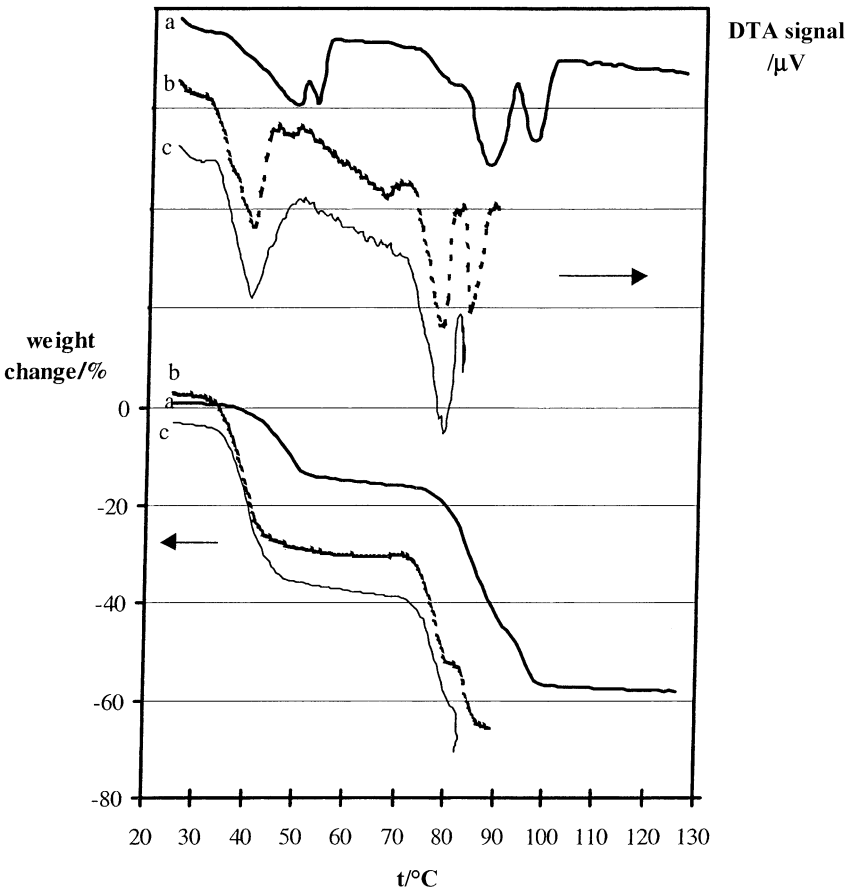

Fig. 1. DTA and weight change curves for the dehydration reaction of $Na_2S{\cdot}xH_2O$ in an atmosphere of helium with 17 mbar water vapour. Heating rate curve a: 1.6 K min^{-1}; curves b and c: 0.4 K min^{-1}.

three dehydration measurements are plotted. The measurements differ in heating rate and in their maximum temperature. It is found that at the highest heating rate (curve a) the first dehydration reaction $Na_2S{\cdot}9H_2O \rightarrow Na_2S{\cdot}5H_2O$ is not completed at the time the sample reaches the melting temperature, 49 °C, of the $Na_2S{\cdot}9H_2O$ phase. Partial melting of the sample occurs, which gives a melting peak in DTA curve a. The same is observed in the next dehydration step from $Na_2S{\cdot}5H_2O \rightarrow Na_2S{\cdot}2H_2O$ where a distinct change in DTA curve a is observed at 83 °C, caused by the melting of some of the $Na_2S{\cdot}5H_2O$ phase. Despite the partial melting of the sample the dehydration reaction still follows the $Na_2S{\cdot}5H_2O \rightarrow Na_2S{\cdot}2H_2O \rightarrow Na_2S{\cdot}\frac{1}{2}H_2O$ sequence, thus a significant part of the sample still is present as a solid phase. This illustrates that a large temperature gradient is present in the sample due to its poor heat conductivity. A lower heating rate of 0.4 K min^{-1} (curves b and c) does not results in melting of the sample. In the weight change curves b and c a small plateau is observed at 80 °C corresponding with the $Na_2S{\cdot}2H_2O$ phase. In one measurement the heating rate was set at 0 K min^{-1}, i.e. kept constant, at $T = 82$ °C (curve c). At this point the dehydration of the $Na_2S{\cdot}2H_2O$ phase started and continued while the temperature was kept constant until the $Na_2S{\cdot}\frac{1}{2}H_2O$ composition was reached. Therefore, DTA curve c in Fig. 1 does not show the last dehydration peak.

Fig. 2 shows the TG curves recorded for the dehydration–rehydration sequence in a flow of helium with 17 mbar water vapour pressure. The weight change as

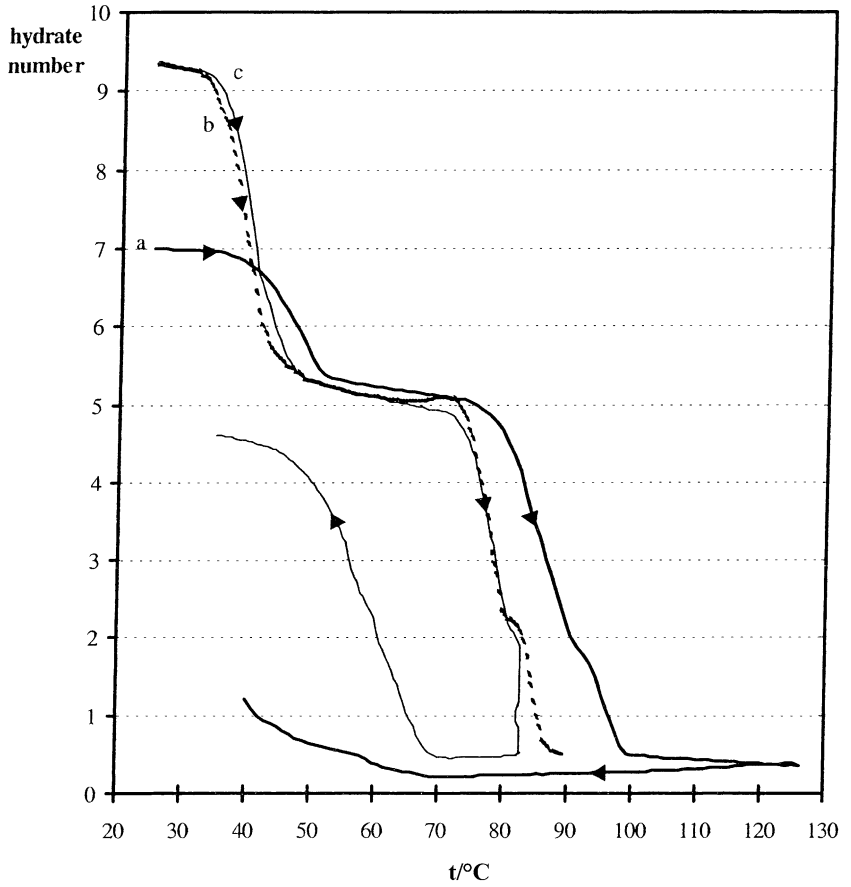

Fig. 2. Rescaled TG curves for the dehydration–rehydration reactions of the $Na_2S{\cdot}xH_2O$ system in an atmosphere of helium wit 17 mbar water vapour. Curve a, heating rate: 1.6 K min^{-1}, cooling rate: 1.6 K min^{-1}; curves b and c, heating and cooling rate: 0.4 K min^{-1}. Rehydration data for curve b were not recorded. Arrows in the curves indicate the direction of change.

function of temperature is scaled to the hydrate number of the sample. The dehydration part is the same as in Fig. 1. Starting compositions of the samples varied due to differences in the equilibration time before the start of a measurement. The measurements at the low heating rate (curves b and c) show a strong overlap and result in the formation of $Na_2S{\cdot}2H_2O$ with a water content slightly higher than that formed with the high heating rate (curve a). The actual water content of $Na_2S{\cdot}2H_2O$ apparently depends on the conditions under which it is formed. It is also obvious from this figure that at high heating and cooling rates the limited heat and mass transfer during the dehydration and rehydration reactions give rise to increased hysteresis. Also the (partial) melting of the sample leads to a more compacted structure which can drastically slow down water vapour uptake. The measurements in an atmosphere of helium with water vapour confirmed the stepwise dehydration from $Na_2S{\cdot}9H_2O$ to $Na_2S{\cdot}5H_2O$ to $Na_2S{\cdot}2H_2O$ and then to $Na_2S{\cdot}\frac{1}{2}H_2O$. Contrary to the experiments in dry helium, where at a low heating rate complete dehydration to anhydrous Na_2S occurs, the presence of some water vapour in the surrounding atmosphere leads to an incompletely dehydrated sodium sulphide. In the rehydration reaction the formation of $Na_2S{\cdot}2H_2O$ was not observed, probably due to kinetic effects of the reactions.

The extrapolated onset temperatures, T_e, of the dehydration and rehydration reactions are given in Table 3 together with the measured enthalpy of reaction. The enthalpy of the dehydration reaction and the rehydration according to reaction (1) was calculated to

Table 3
Extrapolated onset temperatures, T_e, and enthalpies of reaction per mole of dry Na_2S for dehydration and rehydration reactions at $p_{H_2O} = 17$ mbar

Reaction	T_e (°C)	$\Delta_r H$ (kJ mol^{-1})
$Na_2S{\cdot}9H_2O\,(s) \rightarrow Na_2S{\cdot}5H_2O\,(s) + 4H_2O\,(g)$	32.5 ± 1.5	215 ± 20
$Na_2S{\cdot}5H_2O\,(s) \rightarrow Na_2S{\cdot}2H_2O\,(s) + 3H_2O\,(g)$	72.0 ± 1.0	176 ± 12
$Na_2S{\cdot}2H_2O\,(s) \rightarrow Na_2S{\cdot}\frac{1}{2}H_2O\,(s) + 1\frac{1}{2}H_2O\,(g)$	82.0 ± 0.5	94 ± 8
$Na_2S{\cdot}\frac{1}{2}H_2O\,(s) + 4\frac{1}{2}H_2O\,(g) \rightarrow Na_2S{\cdot}5H_2O\,(s)$	71 ± 1	−308 ± 20

be $(2.9 \pm 0.2) \times 10^2$ kJ mol^{-1} of Na_2S. This supports the earlier value of $(3.1 \pm 0.2) \times 10^2$ kJ mol^{-1} of Na_2S determined for the complete dehydration in the atmosphere of dry helium. The hysteresis of the dehydration–rehydration reaction at a heating and cooling rate of 0.4 K min^{-1} is 11 °C, which is larger than that found by Andersson et al. [8], who did the measurements at a heating and cooling rate of 0.05 K min^{-1}.

In the work of Andersson et al. [8,9] expressions for the vapour pressure of $Na_2S{\cdot}5H_2O$ and $Na_2S{\cdot}2H_2O$ are given from which a total heat of reaction is calculated for reaction (1) of 285 kJ mol^{-1} Na_2S, which corroborates the value determined in our work. The dehydration and rehydration reactions of $Na_2S{\cdot}5H_2O$ are described thoroughly in the same work by Andersson et al. It was found that $Na_2S{\cdot}2H_2O$ exists in a temperature range between 60 and 85 °C with a composition varying between $Na_2S{\cdot}2.3H_2O$ and $Na_2S{\cdot}1.6H_2O$. A somewhat disordered crystal structure of $Na_2S{\cdot}2H_2O$ can lead to these variations in its water content. This will be discussed in greater detail in Section 3.3.

3.3. X-ray powder diffraction

The X-ray powder diffraction technique was used primarily for identification of the crystalline phases in the samples during the subsequent decomposition steps. The reference patterns for the known phases were taken from [10–12]. For the study of the dehydration reaction of sodium sulphide hydrate its diffraction pattern was measured while decreasing the water vapour pressure in the helium flow. The sample was kept at 34 °C while the water vapour pressure was slowly reduced from 23 to 9 mbar by slowly reducing the saturator temperature from 20 to 5 °C with 1 °C h^{-1}. At 16 mbar a distinct change in the crystal structure occurs as can be seen in the diffractogram in Fig. 3. The diffraction pattern of $Na_2S{\cdot}9H_2O$ changes into that of $Na_2S{\cdot}5H_2O$.

In a second experiment, using the same sample, the diffraction pattern was recorded while increasing the sample temperature at a rate of 1 °C h^{-1} from 55 to 75 °C. The water vapour pressure was kept constant at 9 mbar. The diffraction pattern of $Na_2S{\cdot}5H_2O$, present at the top of the diffractogram (see Fig. 4) disappears gradually at a sample temperature around 63 °C. A new pattern then arises that corresponds to the phase $Na_2S{\cdot}2H_2O$. On further heating of the sample some small changes are seen in the diffraction pattern of $Na_2S{\cdot}2H_2O$. At a sample temperature of 67 °C the diffraction pattern of Na_2S appears while the diffraction pattern of $Na_2S{\cdot}2H_2O$ gradually fades. The diffraction pattern of $Na_2S{\cdot}2H_2O$ corresponds well with the reported pattern by Andersson and Azoulay [9]. There is clearly no pattern corresponding to an intermediate $Na_2S{\cdot}\frac{1}{2}H_2O$ phase.

From the development of the diffraction pattern of $Na_2S{\cdot}xH_2O$ as a function of the water content a number of interesting observations can be made. All transitions in this so-called crystolysis process [17], show a coexistence region of the higher and lower hydrate; the higher the hydration number the smaller this region. There is no gradual position shift of the diffraction lines that is indicative for the occurrence of a solid solution. Several diffraction lines belonging to one phase appear in the other phase with a different intensity, being indicative for a topotactic transition [17]. The line-width in X-ray diffraction is a measure for the size of the diffracting grains: the smaller the grains the broader the line. No line broadening is observable with this set-up, suggesting no gradual diminishing of the grain size of all grains, during the transition from one hydration state to the other, but a gradual reduction of the number of grains in a

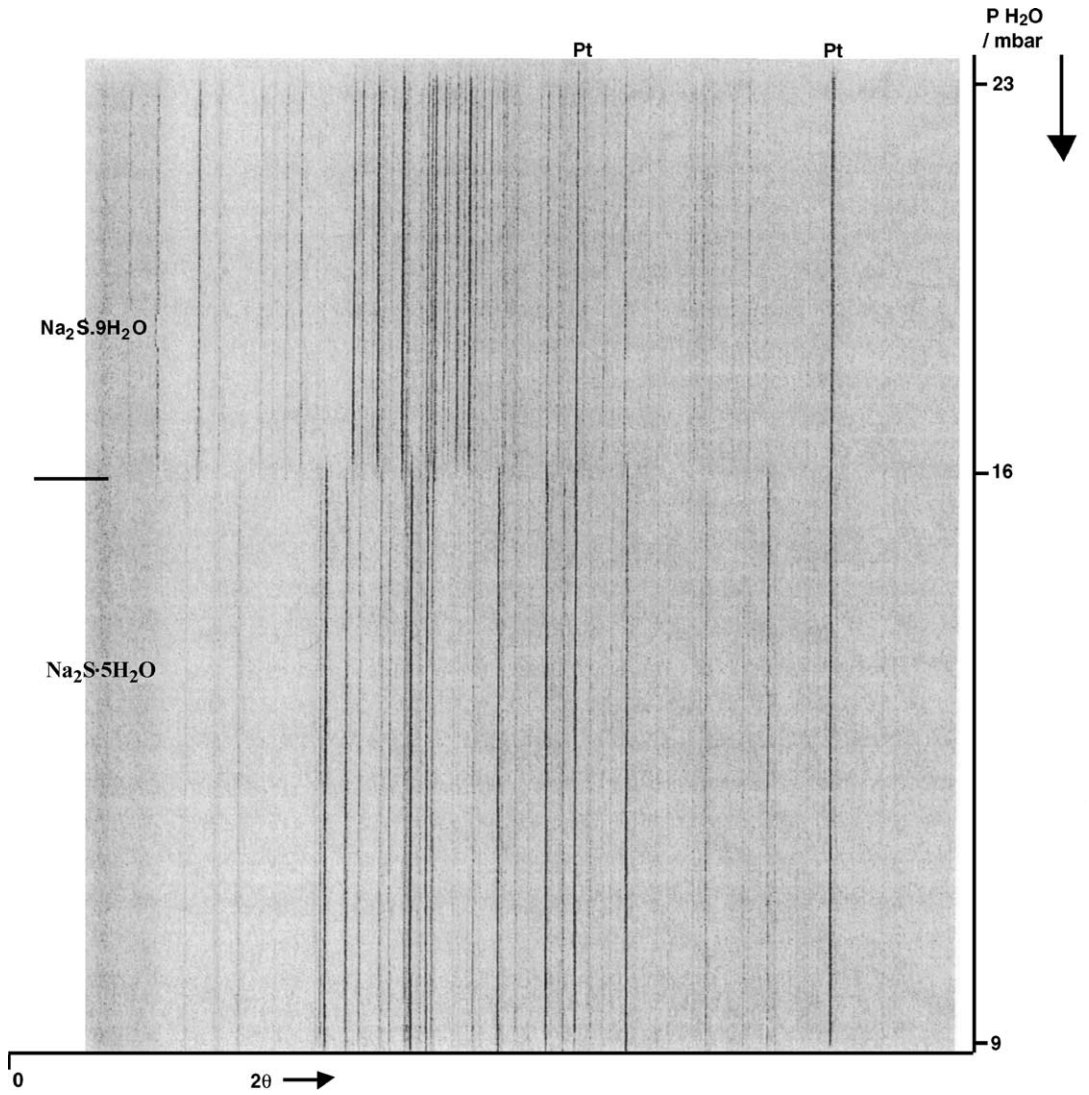

Fig. 3. X-ray diffractogram of $Na_2S{\cdot}xH_2O$ at 34 °C as a function of water vapour pressure in the surrounding atmosphere. At the top of the picture the diffraction pattern of $Na_2S{\cdot}9H_2O$ is present, the bottom part shows the diffraction pattern of $Na_2S{\cdot}5H_2O$. From top to bottom the water vapour pressure decreases from 23 to 9 mbar. Pt indicates the lines arising from the platinum grid used.

specific dehydration state. This is true for all transitions in this system.

Andersson and Azoulay [9], and Mereiter et al. [13] considered the structure of $Na_2S{\cdot}5H_2O$ to consist of alternating layers of sodium, water and sulphur, represented by $\cdots-S-H_2O-Na-H_2O-S-\cdots$. This structure leads to a high mobility of 4 out of 5 water molecules. The transformation of $Na_2S{\cdot}5H_2O$ to $Na_2S{\cdot}2H_2O$ was assumed to be a topotactic process, in which 3 out of 5 water molecules can be removed from the crystal, followed by a shift in the crystallographic position of some of the sodium atoms and the remaining water molecules. This gives a new structure, the $Na_2S{\cdot}2H_2O$ phase. Dehydration of this compound to the anhydrous Na_2S phase was also assumed to occur in a topotactic process.

There is no $Na_2S{\cdot}\frac{1}{2}H_2O$ phase. It is a more or less 'stable' mixture that only exists under mild conditions,

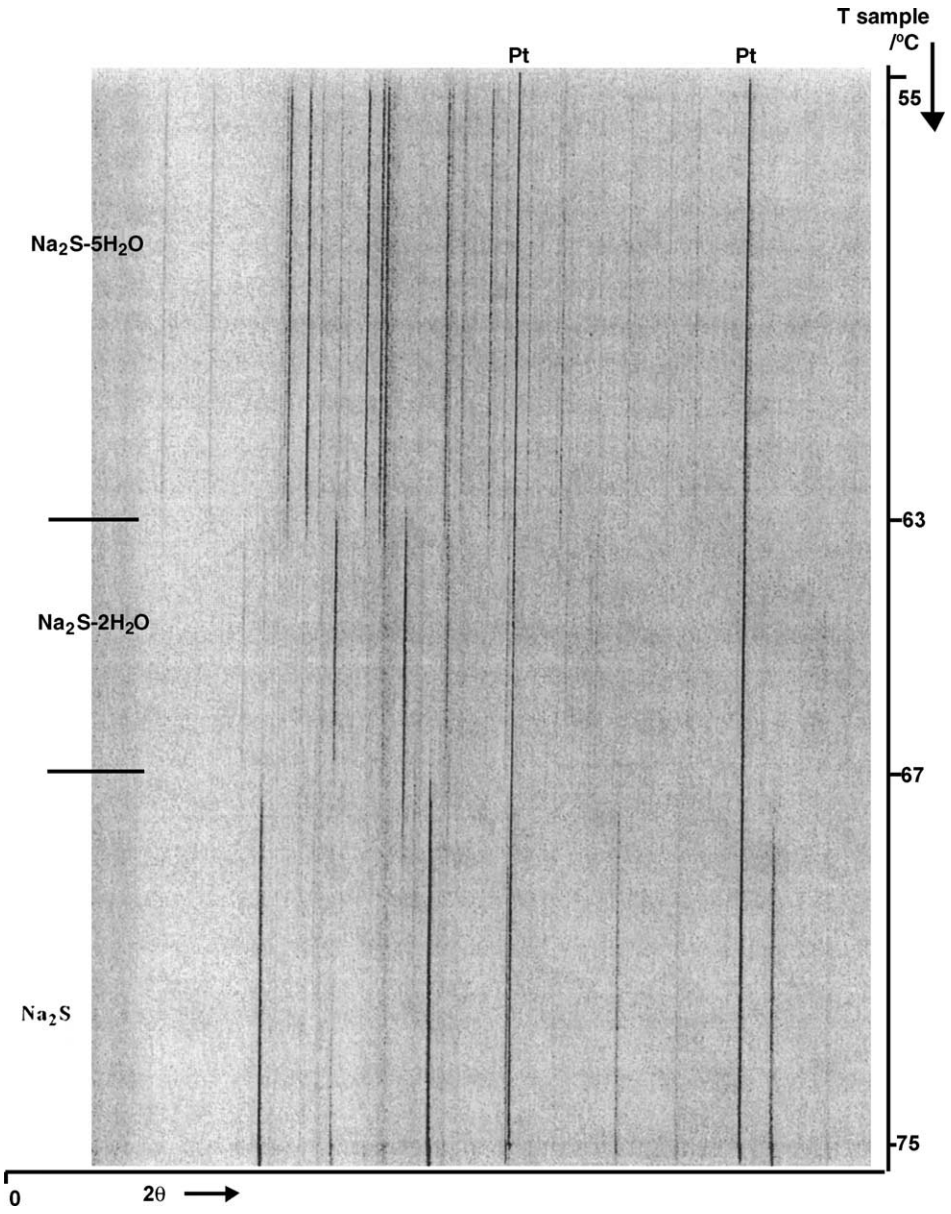

Fig. 4. X-ray diffractogram of $Na_2S{\cdot}xH_2O$ as a function of sample temperature. The water vapour pressure in the surrounding atmosphere was 9 mbar. At the top of the picture the diffraction pattern of $Na_2S{\cdot}5H_2O$ in present, the bottom part shows the diffraction pattern of anhydrous Na_2S. From top to bottom the sample temperature increases from 55 to 75 °C. Pt indicate the diffraction lines arising from the platinum grid used.

presumably due to slow kinetics of the dihydrate particles in the anhydrous matrix. Dehydration at $t > 350$ °C under high vacuum yields pure Na_2S that does no longer react with water vapour [18].

3.4. Phase diagram

The results of the melting point determinations using DTA on samples of sodium sulphide hydrate

Table 4
Results of the DTA measurements and melting point determinations

Sample composition	Mole fraction Na_2S	DTA transition temperatures (°C)			T_{melt} (°C)
$Na_2S{\cdot}3.24H_2O$	0.24	75 ± 1	89 ± 1		83.6 ± 0.2
$Na_2S{\cdot}3.0H_2O$	0.25	74 ± 1	80 ± 1	92 ± 1	83.7 ± 0.2
$Na_2S{\cdot}1.8H_2O$	0.36	75 ± 1	80 ± 1	92 ± 1	82.9 ± 0.2
$Na_2S{\cdot}0.93H_2O$	0.52	74 ± 1	80 ± 1	92 ± 1	83.4 ± 0.2

are given in Table 4. The transition temperatures however, were only determined on heating the sample. On cooling the sample, effects of supercooling prevented a reproducible measurement. The transition temperatures were determined using extrapolated onset temperatures. Due to reactions of the molten sample with the glass capsule, transition temperatures were taken only at the first heating. In subsequent heating runs the transition temperatures were shifted and the enthalpy effect had decreased. Already before the first measurement the sample was molten shortly during sealing of the capsule. A small part of the sample could have been contaminated prior to the actual measurement, leading to additional heat effects (pre-melting). To avoid effects of contamination of the sample more accurate melting point determinations were done using tubular glass capsules that were much larger in order to prevent the melting of the sample on sealing the capsule. The results of these measurements are given in the last column of Table 4.

The results of the TG/DTA experiments (see Sections 3.1 and 3.2), the DTA measurements and the melting point determinations are plotted together into the phase diagram of the Na_2S–H_2O system (Fig. 5).The first description of the Na_2S–H_2O system was given by Kopylov [6] and recently extended with the high temperature section by Kopylov and Kaminski [7]. The results of our melting point measurements correspond to the determinations of Kopylov and Kaminski. The main difference as deduced from our X-ray determinations is that the phase $Na_2S{\cdot}\frac{1}{2}H_2O$ reported by Kopylov and Kaminski [7]

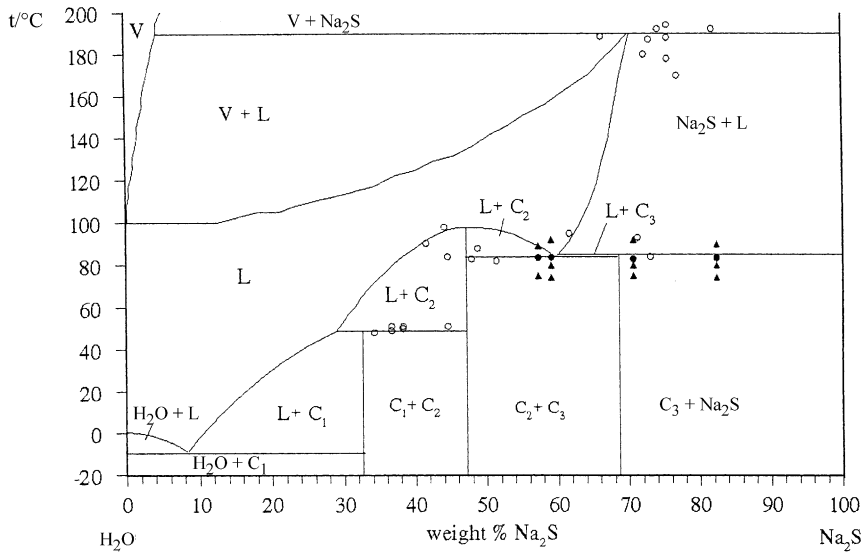

Fig. 5. Phase diagram of the Na_2S–H_2O system (based on [6,7]) and measured transition temperatures: ▲, represent results of the DTA measurement; ●, are the results of the melting point determinations; ○, represent the transition temperatures measured by the TG/DTA experiments presented in Section 3.1. Phase denominations: V, vapour; L, H_2O based solution; C_1, C_2 and C_3 are the crystalline phases $Na_2S{\cdot}9H_2O$, $Na_2S{\cdot}5H_2O$, and $Na_2S{\cdot}2H_2O$, respectively.

Table 5
Results of the vapour pressure measurements of water

T (°C)	p_{H_2O} (10^2 Pa)		Difference (10^2 Pa)	Difference (%)
	Experimental	Reference [19]		
9.99	12.87	12.27	0.61	4.95
14.95	17.35	17.01	0.33	1.96
14.92	17.70	16.98	0.72	4.25
14.95	17.17	17.01	0.15	0.90
15.00	17.24	17.07	0.17	1.01
24.89	31.46	31.48	−0.02	−0.06
24.89	31.54	31.48	0.07	0.21
34.73	54.70	55.43	−0.73	−1.32
34.80	56.11	55.64	0.47	0.84
39.89	73.21	73.37	−0.15	−0.21
39.93	73.04	73.56	−0.52	−0.71
43.59	88.12	89.18	−1.07	−1.19
43.56	87.76	89.04	−1.28	−1.44

is now replaced by $Na_2S{\cdot}2H_2O$. Furthermore it is seen that the presence of the $Na_2S{\cdot}2H_2O$ phase does not lead to significant changes in the melting temperature for samples with compositions between $Na_2S{\cdot}5H_2O$ and $Na_2S{\cdot}\frac{1}{2}H_2O$. At 83 °C melting of sodium sulphide hydrate for the aforementioned compositions occurs. This means that for a chemical heat pump, using Na_2S–H_2O as working pair, regeneration temperatures cannot exceed 83 °C without melting part of the salt hydrate.

The present study does not confirm the existence of the compound $Na_2S{\cdot}\frac{1}{2}H_2O$: the TG/DTA measurements yield varying compositions for the ''dehydrated'' sodium sulphide ranging from $Na_2S{\cdot}0.9H_2O$ to Na_2S, dependent on the reaction conditions. Andersson and Azoulay [9] assumed that the residual water content was caused by the stabilisation of a small amount of the $Na_2S{\cdot}2H_2O$ phase in the dehydrated Na_2S phase.

3.5. Vapour pressure measurements

The results of the vapour pressure measurements are summarised in Table 5 through Table 8. First the vapour pressure of pure water was measured to check the performance of the experimental set-up. The result of these measurements (Table 5) shows that vapour pressures can be determined with an accuracy of approximately 2%. The vapour pressure measurements on a sample of $Na_2S{\cdot}9H_2O$ gave the results as shown in Table 6.

For the vapour pressure measurements on $Na_2S{\cdot}5H_2O$ two different samples were used in order to check the reproducibility of the measurement. The results of both measurement are put together in Table 7. The vapour pressure of $Na_2S{\cdot}2H_2O$ was also determined on two samples in the same way as with $Na_2S{\cdot}5H_2O$. The results of these measurements are compiled in Table 8.

In Fig. 6 the results of the measurements are displayed graphically together with the calculated functions for the water vapour pressure of the three sodium sulphide hydrates. This function is based on the Van't Hoff equation for the vapour pressure of a substance. The limited accuracy of the measurement does not allow for a more detailed description of the vapour

Table 6
Results of the vapour pressure measurements of $Na_2S{\cdot}9H_2O$

T (°C)	p_{H_2O} (10^2 Pa)
4.99	2.19
5.06	2.28
14.92	5.10
14.97	5.15
16.99	6.11
24.92	11.11
24.92	11.04
34.83	22.91
34.83	22.77
43.61	41.41
43.61	41.39

Table 7
Results of the vapour pressure measurements of $Na_2S{\cdot}5H_2O$

T (°C)	p_{H_2O} (10^2 Pa)
14.97	0.32
14.97	0.25
14.97	0.27
24.92	0.60
24.92	0.53
24.92	0.46
34.80	1.28
34.88	0.99
34.90	1.29
44.77	2.85
54.73	6.32
54.78	5.88
54.81	6.26
54.83	4.73
64.78	12.44
69.68	17.28
69.81	14.30
74.71	23.80
82.59	38.48

Table 8
Results of the vapour pressure measurements of $Na_2S{\cdot}2H_2O$

T (°C)	p_{H_2O} (10^2 Pa)
5.04	0.02
14.97	0.08
24.92	0.22
29.82	0.23
34.88	0.82
34.88	0.59
39.86	0.74
43.64	1.30
43.64	1.21
49.75	2.45
49.75	1.66
59.74	4.68
59.77	4.02
69.60	8.99
69.76	8.18
79.75	15.66

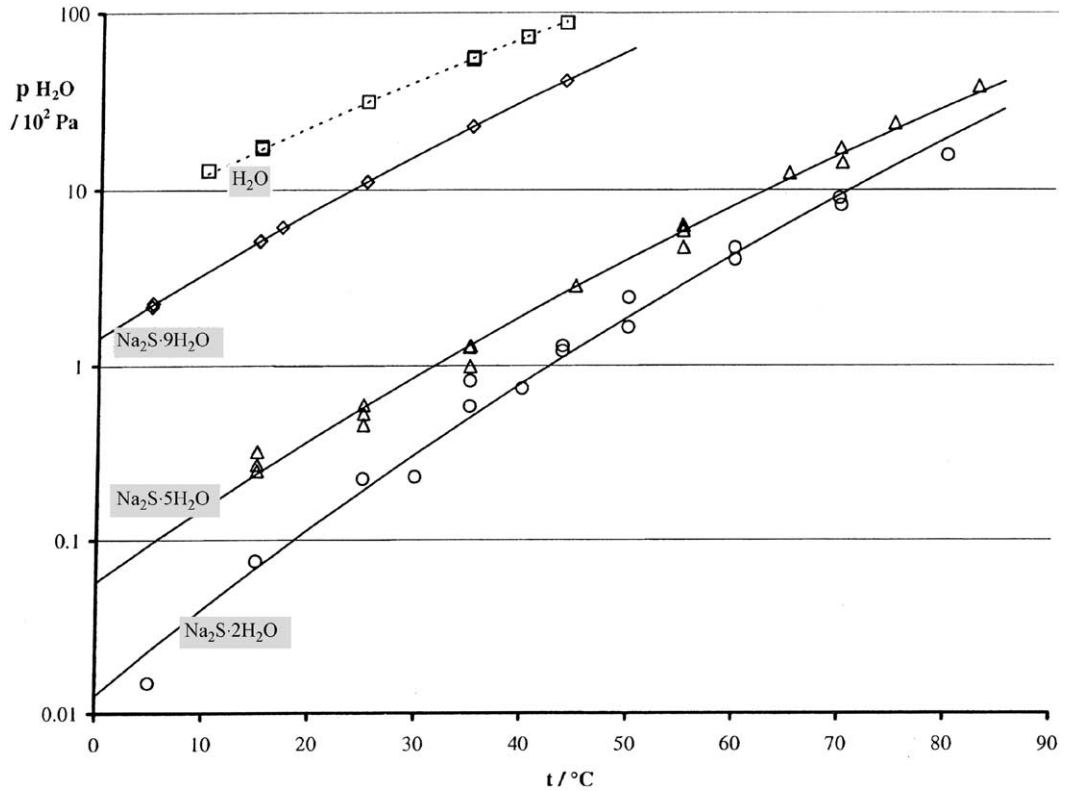

Fig. 6. Results of the vapour pressure measurements on water and sodium sulphide hydrates. (□) H_2O; (◇) $Na_2S{\cdot}9H_2O$; (△) $Na_2S{\cdot}5H_2O$; (○) $Na_2S{\cdot}2H_2O$. The solid lines represent the calculated Van't Hoff equation for the vapour pressure of the indicated salt hydrates.

Table 9
Calculated enthalpy and entropy of the dehydration reactions of sodium sulphide hydrates

Reaction	$\Delta_r H$ (kJ mol^{-1})	$\Delta_r H$ (kJ mol^{-1} H_2O)	$\Delta_r S$ (J mol^{-1} K^{-1})	$\Delta_r S$ (J mol^{-1} H_2O K^{-1})
$Na_2S{\cdot}2H_2O$ (s) → Na_2S (s) + $2H_2O$ (g)	148 ± 10	74 ± 5	353 ± 33	177 ± 16
$Na_2S{\cdot}5H_2O$ (s) → $Na_2S{\cdot}2H_2O$ (s) + $3H_2O$ (g)	189 ± 8	63 ± 3	447 ± 26	149 ± 9
$Na_2S{\cdot}9H_2O$ (s) → $Na_2S{\cdot}5H_2O$ (s) + $4H_2O$ (g)	222 ± 2	55.4 ± 0.4	592 ± 4	148 ± 1

pressure, e.g. by means of the method described by Oonk et al. [20] that takes into account the change in heat capacity of the reactants and the products.

The results of the vapour pressure measurement are used to calculate the change in enthalpy and entropy of the dehydration reactions by means of the Van't Hoff equation, expressed per mole of water:

$$\ln\frac{p}{p^\circ} = \frac{\Delta_r S}{R} - \frac{\Delta_r H}{R \cdot T}$$

with $p^\circ = 1$ bar and $R = 8.3145$ J mol^{-1} K^{-1}.

The calculated enthalpy and entropy of the reactions are given in Table 9. The reported errors are derived from the least squares fit of the measurements to the Van't Hoff equation and represent 95% confidence limits.

The values of $\Delta_r H$ and $\Delta_r S$ increase with decreasing water content as can be expected: the lower the hydration number the stronger the water molecule is bound. In Table 10 a comparison is made between the derived enthalpies and entropies of reaction with the literature values from [9]. A difference of less than 7% is found for the enthalpy of the reactions but a much larger difference is observed for the entropy of the reactions. The values of 200 J mol^{-1} K^{-1} for the reactions is given by Andersson and Azoulay [9] seem to be too high considering that the standard entropy of pure water vapour is 188 J mol^{-1} K^{-1}.

In Fig. 7 the results of the direct vapour pressure measurements are compared with the results of indirect determinations of vapour pressure equilibria in TG/DTA and XRD experiments. The latter are derived from the transition temperatures observed while heating a $Na_2S{\cdot}xH_2O$ sample in a flow of helium with a constant known water vapour pressure. A good agreement is found between the different types of measurements. The TG/DTA and XRD results suggest a slightly lower vapour pressure for the respective compounds, but the dynamic character of these measuring methods can give rise to slightly higher transition temperatures.

The vapour pressure data of Andersson and Azoulay [9] are also plotted in Fig. 7, and illustrate that their TG/DTA results are in close agreement with our data. The vapour pressure functions determined by Andersson, in the figure indicated by the dashed lines, show a deviation of a few degrees Celsius from the functions determined in this study. The reason in the case of $Na_2S{\cdot}2H_2O$ is that Andersson took the average value from dynamic measurements of dehydration and rehydration. Our data are based purely on static equilibrium measurements, as are the experimental points from [9] indicated by the solid symbols. The equilibrium data are to be preferred.

3.6. Calculation of the thermodynamic functions of sodium sulphide hydrates

In Table 11 the calculated enthalpy of formation of the three crystalline sodium sulphide hydrates are

Table 10
Comparison between enthalpy and entropy of reaction in this study with literature values [9]

Reaction	$\Delta_r H$ (kJ mol^{-1} H_2O)			$\Delta_r S$ (J mol^{-1} H_2O K^{-1})		
	This study	[9]	Difference (%)	This study	[9]	Difference (%)
$Na_2S{\cdot}2H_2O$ (s) → Na_2S (s) + $2H_2O$ (g)	−73.9	−69.0	6.6	177	220	24
$Na_2S{\cdot}5H_2O$ (s) → $Na_2S{\cdot}2H_2O$ (s) + $3H_2O$ (g)	−62.9	−60.6	3.6	149	199	34

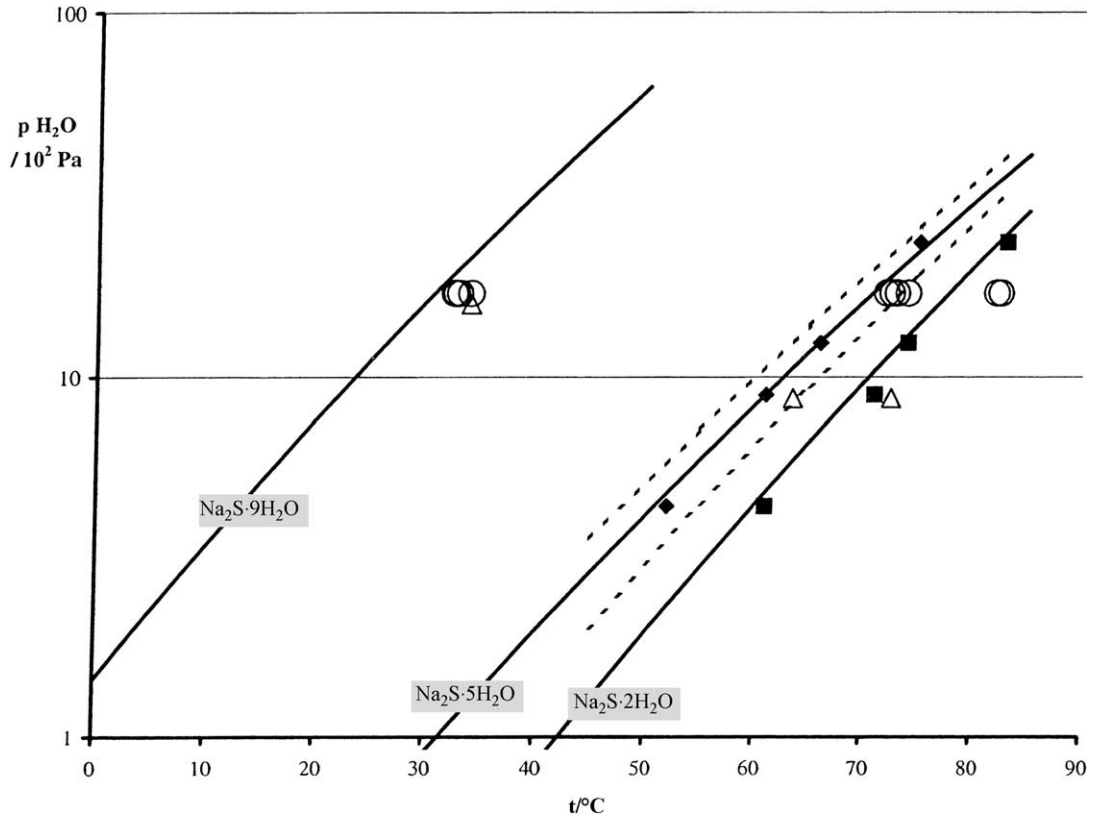

Fig. 7. A comparison between the calculated vapour pressure functions and the results of TG/DTA measurements, XRD measurements, and data from [9]. Solid lines represent the calculated vapour pressure functions of the indicated sodium sulphide hydrates. (○) TG/DTA; (△) XRD; solid symbols are TG/DTA results of [9] and the dashed lines represent the vapour pressure functions from [9].

compared to literature values. The enthalpy of formation of $Na_2S{\cdot}2H_2O$ is calculated using the enthalpy of formation of the reaction products, Na_2S and H_2O and the measured enthalpy of the reaction

$$\Delta_f H^\circ\,(Na_2S \cdot 2H_2O\,(s)) = 2\Delta_f H^\circ\,(H_2O\,(g)) + \Delta_f H^\circ\,(Na_2S\,(s)) + \Delta_r H$$

The enthalpies of formation of the other sodium sulphide hydrates are calculated in a similar way. The calculated and earlier reported literature values agree very well.

The enthalpy and entropy of the equilibrium reactions given in Table 9 are also used to calculate the thermodynamic functions of the sodium sulphide hydrates. The well-known thermodynamic functions of H_2O (g) [22] and Na_2S [23] are also used for this calculation.

The enthalpy of $Na_2S{\cdot}2H_2O$ at each temperature is calculated from the enthalpies of the reaction

Table 11
Calculated enthalpies of formation of the sodium sulphide hydrates and a comparison with literature values

Compound	$\Delta_f H^\circ$ (298.15) (kJ mol^{-1}), this study	$\Delta_f H^\circ$ (298.15) (kJ mol^{-1}), [21]	Difference	
			kJ mol^{-1}	%
$Na_2S{\cdot}2H_2O$	−998	–	–	–
$Na_2S{\cdot}5H_2O$	−1912	−1886.6	−25	1.3
$Na_2S{\cdot}9H_2O$	−3101	−3074.0	−27	0.9

Table 12
Heat capacity, C_p, entropy, S°, and Gibbs energy of formation, $\Delta_f G^\circ$, of the sodium sulphide hydrates

Compound	$C_p = A + B \cdot T$		S° (298.15) (J mol^{-1} K^{-1})	$\Delta_f G^\circ$ (298.15) (kJ mol^{-1})
	A (J mol^{-1} K^{-1})	B (J mol^{-1} K^{-1})		
$Na_2S{\cdot}2H_2O$	142.4	2.562×10^{-2}	120.3	−855
$Na_2S{\cdot}5H_2O$	238.3	4.197×10^{-2}	239.4	−1596
$Na_2S{\cdot}9H_2O$	370.7	4.875×10^{-2}	400.5	−2555

products, Na_2S and H_2O and the measured enthalpy of the reaction. For the entropy of $Na_2S{\cdot}2H_2O$ the same procedure is applied, using the entropies of the reaction products and the measured entropy of the reaction. The heat capacity, C_p, of the sodium sulphide hydrates is calculated from the sum of the heat capacities of water vapour and Na_2S and fitted with the relation

$$C_p = A + B \cdot T$$

where A and B are constants and T the temperature in Kelvin. In Table 12 the values for A and B are given together with the standard entropy and the Gibbs energy of formation.

The Gibbs energy of the sodium sulphide hydrates is simply calculated from the enthalpy and the entropy. The thermodynamic functions of $Na_2S{\cdot}2H_2O$ and similarly derived for $Na_2S{\cdot}5H_2O$ and $Na_2S{\cdot}9H_2O$, are given in Tables 13–15. The equilibrium reactions given in Table 9 are used for the calculation.

Table 13
Thermodynamic functions of $Na_2S{\cdot}2H_2O$

Temperature T /K	Heat capacity $C_{p,\,m}$/J mol^{-1} K^{-1}	Entropy S°_m/J mol^{-1} K^{-1}	Enthalpy H°_m/kJ mol^{-1}	Gibbs energy G°_m/kJ mol^{-1}
273.15	*149.4*[a]	*107.2*	*−1001.2*	*−1031*
278.15	*149.5*	*109.9*	*−1000.5*	*−1031*
283.15	*149.6*	*112.6*	*−999.7*	*−1032*
288.15	149.7	115.2	−999.0	−1032
293.15	149.9	117.8	−998.2	−1033
298.15	150.0	120.3	−997.5	−1033
303.15	150.1	122.8	−996.7	−1034
308.15	150.3	125.3	−996.0	−1035
313.15	150.4	127.7	−995.2	−1035
318.15	150.5	130.1	−994.5	−1036
323.15	150.6	132.4	−993.7	−1037
328.15	150.8	134.7	−993.0	−1037
333.15	150.9	137.0	−992.2	−1038
338.15	151.0	139.2	−991.5	−1039
343.15	151.2	141.5	−990.7	−1039
348.15	151.3	143.7	−990.0	−1040
353.15	151.4	145.8	−989.2	−1041
358.15	*151.5*	*147.9*	*−988.4*	*−1041*
363.15	*151.7*	*150.0*	*−987.7*	*−1042*
368.15	*151.8*	*152.1*	*−986.9*	*−1043*
373.15	*151.9*	*154.2*	*−986.2*	*−1044*

Nomenclature in accordance with SGTE (Scientific Group Thermodata Europe): $S^\circ_m = \Delta^T_0 S^\circ_m = \int_0^T \frac{C_{P,m}}{T} dT$, $H^\circ_m = \Delta_f H^\circ_m(298.15\,K) + \int_{298.15}^T C_{P,m} dT$, $G^\circ_m = H^\circ_m - TS^\circ_m$

[a] Figures in italic are extrapolated.

Table 14
Thermodynamic functions of $Na_2S·5H_2O$

Temperature T /K	Heat capacity $C_{p,m}$/J mol^{-1} K^{-1}	Entropy S°_m/J mol^{-1} K^{-1}	Enthalpy H°_m/kJ mol^{-1}	Gibbs energy G°_m/kJ mol^{-1}
273.15	*249.7*[a]	*217.4*	*−1918*	*−1977*
278.15	*250.0*	*222.0*	*−1917*	*−1978*
283.15	*250.2*	*226.4*	*−1915*	*−1980*
288.15	250.4	230.8	−1914	−1981
293.15	250.6	235.1	−1913	−1982
298.15	250.8	239.4	−1912	−1983
303.15	251.0	243.6	−1910	−1984
308.15	251.2	247.7	−1909	−1985
313.15	251.4	251.7	−1908	−1987
318.15	251.6	255.7	−1907	−1988
323.15	251.8	259.6	−1905	−1989
328.15	252.1	263.5	−1904	−1991
333.15	252.3	267.3	−1903	−1992
338.15	252.5	271.0	−1902	−1993
343.15	252.7	274.8	−1900	−1995
348.15	252.9	278.4	−1899	−1996
353.15	253.1	282.0	−1898	−1997
358.15	253.3	285.6	−1897	−1999
363.15	*253.5*	*289.1*	*−1895*	*−2000*
368.15	*253.7*	*292.6*	*−1894*	*−2002*
373.15	*253.9*	*296.0*	*−1893*	*−2003*

Nomenclature in accordance with SGTE (Scientific Group Thermodata Europe): $S^\circ_m = \Delta^T_0 S^\circ_m = \int^T_0 \frac{C_{P,m}}{T} dT, H^\circ_m = \Delta_f H^\circ_m(298.15\,K) + \int^T_{298.15} C_{P,m} dT, G^\circ_m = H^\circ_m - TS^\circ_m$

[a] Figures in italic are extrapolated.

Table 15
Thermodynamic functions of $Na_2S·9H_2O$

Temperature T /K	Heat capacity $C_{p,m}$/J mol^{-1} K^{-1}	Entropy S°_m/J mol^{-1} K^{-1}	Enthalpy H°_m/kJ mol^{-1}	Gibbs energy G°_m/kJ mol^{-1}
273.15	*384.0*[a]	*366.8*	*−3110*	*−3210*
278.15	384.3	373.8	−3108	−3212
283.15	384.5	380.6	−3106	−3214
288.15	384.8	387.4	−3104	−3216
293.15	385.0	394.0	−3103	−3218
298.15	385.2	400.5	−3101	−3220
303.15	385.5	406.9	−3099	−3222
308.15	385.7	413.2	−3097	−3224
313.15	386.0	419.4	−3095	−3226
318.15	386.2	425.5	−3093	−3228
323.15	*386.5*	*431.6*	*−3091*	*−3230*

Nomenclature in accordance with SGTE (Scientific Group Thermodata Europe): $S^\circ_m = \Delta^T_0 S^\circ_m = \int^T_0 \frac{C_{P,m}}{T} dT, H^\circ_m = \Delta_f H^\circ_m(298.15\,K) + \int^T_{298.15} C_{P,m} dT, G^\circ_m = H^\circ_m - TS^\circ_m$

[a] Figures in italic are extrapolated.

4. Conclusion

In the Na_2S–H_2O system the existence of the compounds $Na_2S·9H_2O$, $Na_2S·5H_2O$ and Na_2S has been confirmed by TG/DTA and XRD techniques. In addition the existence of a new phase of composition $Na_2S·2H_2O$ has been proven as a fact. Furthermore the compound with composition $Na_2S·\frac{1}{2}H_2O$ is not a

genuine phase but is a 1:3 mixture of Na_2S and $Na_2S{\cdot}2H_2O$ (Fig. 5). The kinetics of the reaction of $Na_2S{\cdot}2H_2O$ to Na_2S in small domains of the dihydrate is so slow that under mild conditions this composition appears to be stable. The reaction enthalpy and entropy of the pentahydrate to the dihydrate as well as of the dihydrate to dry sodium sulphide transitions have been established. The water vapour pressure as a function of temperature of all three hydrates has been determined and based on these measurements a consistent set of thermodynamic functions for the sodium sulphide hydrates is calculated. The melting temperature of $Na_2S{\cdot}9H_2O$ is 49 °C and mixtures of $Na_2S{\cdot}5H_2O$ with $Na_2S{\cdot}2H_2O$ and of $Na_2S{\cdot}2H_2O$ with Na_2S melt at 83 °C.

The results of the experiments are in good agreement with earlier work on the crystallographic, physical and thermochemical properties of the Na_2S–H_2O system [6–13]. As to the exact composition of the 'dihydrate' it is recommended to perform neutron or X-ray diffraction experiments to elucidate the crystal structure.

For utilisation of the Na_2S–H_2O system as working pair in a solid-sorption type chemical heat pump with integrated heat or cold storage function, the operating window has been established. The melting temperature of the salt hydrate in the composition range between $Na_2S{\cdot}5H_2O$ and $Na_2S{\cdot}\frac{1}{2}H_2O$ is 83 °C. The heat storage capacity based on the dehydration reaction of the salt is

$$Na_2S \cdot 5H_2O\,(s) \rightarrow Na_2S \cdot \tfrac{1}{2}H_2O\,(s) + 4\tfrac{1}{2}H_2O\,(g),$$
$$\Delta_r H\,(298.15\,K, 1\,bar) = 300 \pm 15\,kJ\,mol^{-1} \qquad (2)$$

This equals 3.84 MJ kg^{-1} Na_2S or approximately 1 kWh kg^{-1} Na_2S. One mole of Na_2S can absorb $4\frac{1}{2}$ moles of water, which is equal to the absorption of 1 kg of water in 1 kg of dry salt. The theoretical cold storage capacity of this working pair, based on the heat of evaporation of water is 2.54 MJ kg^{-1} Na_2S.

Acknowledgements

Mr. R.G. Nyqvist (Thermal Analysis) and Mr. P. van Vlaanderen (X-ray diffraction) are acknowledged for painstakingly performing these measurements. SWEAT BV and the Netherlands Agency for Energy and the Environment (NOVEM) are gratefully acknowledged for financial support.

References

[1] J.A. Carp, P.W. Bach, Energy Research Centre of the Netherlands, P.O. Box 1, 1755 ZG Petten, The Netherlands, personal communication on European Waste Heat Potential, (2000).
[2] C. Schweigler, S. Summerer, H.-M. Hellmann, F. Ziegler (Eds.), Proceedings of the International Sorption Heat Pump Conference, Munich, Germany, March 24–26, 1999.
[3] G. Restuccia, J.A. Arnoud, R. Quagliata, Int. J. Energy Res. 12 (1) (1988) 101.
[4] V. Goetz, A. Marty, Calorimetrie et Analyse Thermique 23 (1992) 431.
[5] Z. Tamainot-Telto, R.E. Critoph, Appl. Therm. Eng. 21 (2001) 37.
[6] N.I. Kopylov, Russ. J. Inorg. Chem. 13 (2) (1968) 276.
[7] N.I. Kopylov, Yu.V. Kaminski, Russ. J. Inorg. Chem. 44 (2) (1999) 261.
[8] J.Y. Andersson, J. de Pablo, M. Azoulay, Thermochim. Acta 91 (1985) 223.
[9] J.Y. Andersson, M. Azoulay, J. Chem. Soc. Dalton Trans. 3 (1986) 469.
[10] JCPDS-ICDD Powder Diffraction File, International Centre for Diffraction Data, 12 Campus Boulevard, Newtown Square, PA 19073-3273 USA, 1997.
[11] D. Bedlivy, A. Preisinger, Zeitschrift für Kristallografie 121 (1965) 114.
[12] D. Bedlivy, A. Preisinger, Zeitschrift für Kristallografie 121 (1965) 135.
[13] K. Mereiter, A. Preisinger, A. Zellner, W. Mikenda, H. Steidl, J. Chem. Soc. Dalton Trans. 7 (1984) 1275.
[14] S. Andersson, Chem. Scripta 20 (1982) 164.
[15] Reference materials for Thermal analysis GM 758, Certified by the International Confederation for Thermal Analysis, distributed by the US National Bureau of Standards (today NIST, USA), 1971.
[16] R. Riesen, G. Wiedmann, Thermoanalyse, Dr Alfred Hüthing Verlag GmbH, Heidelberg, 1984.
[17] A.K. Galwey, Thermochim. Acta 355 (2000) 181.
[18] W.G. Haije, R. de Boer, Unpublished results of failed chemisorption experiments on dry Na_2S.
[19] D.R. Lide (Ed.), Handbook of Chemistry and Physics, 78th Edition, CRC Press, New York, 1997.
[20] H.A.J. Oonk, P.R. van der Linde, J. Huinink, J.G. Blok, J. Chem. Thermodyn. 30 (1998) 897.
[21] D.D. Wagman, W.H. Evans et al., J. Phys. Chem. Ref. Data 11 (1982) 306.
[22] J.D. Cox, D.D. Wagman, V.A. Medvedev, CODATA Key Values for Thermodynamics, Hemisphere, New York, 1989.
[23] M.W. Chase Jr., C.A. Davies et al., J. Phys. Chem. Ref. Data 14 (1985) 1595.